

Article

Supercritical CO₂ Foaming of Poly(3-hydroxybutyrate-co-4-hydroxybutyrate)

Tao Zhang ¹, Yunjae Jang ², Eunhye Lee ², Sooan Shin ² and Ho-Jong Kang ^{1,*} 

¹ Department of Polymer Science and Engineering, Dankook University, 152 Jukjeon-ro, Suji-gu, Yongin-si 16890, Gyeonggi-do, Korea; taozhang1214@gmail.com

² CJ Cheiljedang Corporation, 55 Gwanggyo-ro, 42 beon-gil, Yeongtong-gu, Suwon-si 16495, Gyeonggi-do, Korea; yunjae.jang@cj.net (Y.J.); eunhye.lee@cj.net (E.L.); sooanshin@gmail.com (S.S.)

* Correspondence: hjkang@dankook.ac.kr

Abstract: The supercritical carbon dioxide foaming characteristics of the biodegradable polymer poly(3-hydroxybutyrate-co-4-hydroxybutyrate) (P(3HB-co-4HB)) are studied for environmentally friendly packaging materials. The effect of the 4HB composition of the P(3HB-co-4HB) copolymers on the foaming conditions such as pressure and temperature is studied and the density and the expansion ratio of the resulting P(3HB-co-4HB) foam are together evaluated. The increase in the 4HB content reduces the crystallinity and $\tan \delta$ value of P(3HB-co-4HB) required for the growth of the foam cells. Therefore, the foaming temperature needs to be lower to retain a suitable $\tan \delta$ value of P(3HB-co-4HB) for foaming. It was found that P(3HB-co-4HB) with less crystallinity showed better formability and cell uniformity. However, foaming is not possible regardless of the foaming temperature when the 4HB content of P(3HB-co-4HB) is over 50%, due to the high $\tan \delta$ value. A lower foam density and higher expansion ratio can be obtained with crystalline P(3HB-co-4HB) of low 4HB content, compared with non-crystalline P(3HB-co-4HB) of high 4HB content. The expansion ratio of P(3HB-co-4HB) foams can be increased slightly by using a chain extender, due to the lowering of crystallinity and $\tan \delta$. This is most effective in the case of P(3HB-co-4HB), whose 4HB content is 16%.

Keywords: poly(3-hydroxybutyrate-co-4-hydroxybutyrate); supercritical carbon dioxide; P(3HB-co-4HB) foams; expansion ratio; chain extender



Citation: Zhang, T.; Jang, Y.; Lee, E.; Shin, S.; Kang, H.-J. Supercritical CO₂ Foaming of Poly(3-hydroxybutyrate-co-4-hydroxybutyrate). *Polymers* **2022**, *14*, 2018. <https://doi.org/10.3390/polym14102018>

Academic Editor: Alberto Romero García

Received: 28 March 2022

Accepted: 10 May 2022

Published: 15 May 2022

Publisher's Note: MDPI stays neutral with regard to jurisdictional claims in published maps and institutional affiliations.



Copyright: © 2022 by the authors. Licensee MDPI, Basel, Switzerland. This article is an open access article distributed under the terms and conditions of the Creative Commons Attribution (CC BY) license (<https://creativecommons.org/licenses/by/4.0/>).

1. Introduction

Polyhydroxyalkanoates (PHAs) are biodegradable polymers produced by microorganisms and have very wide applicability as an alternative material for synthetic polymers, which cause environmental pollution as they are degraded under diverse earth environments, contrary to other biodegradable polymers [1,2]. Due to their excellent biocompatibility and in vivo degradation properties, their application is being extended to medical materials [3]. The developed PHA products are melt processed films [4,5] or foams [6] for environmentally friendly packing material and research is being carried out regarding their application to medical materials, such as biodegradable sutures from electrospinning [7] and scaffolds for tissue engineering from 3D printing [8], etc.

Poly(3-hydroxybutyrate) (P3HB) was the first biodegradable polymer to be studied among the PHAs, but had the limitation of having a narrow window for melt processing, as thermal degradation occurs very easily [9]. Furthermore, its crystallization rate is very low, resulting in large spherulites with the interface among these resulting in brittleness and the crystallization continually occurs during solidification, making the stable production of molded products difficult [10]. To overcome these problems, blending with biodegradable polymers that are compatible with P3HB, such as polylactic acid (PLA) and polybutylene succinate (PBS) [11,12], modification of the structure by branching or crosslinking

through the addition of diverse additives [13,14], and the bacterial synthesis of copolymers from biodegradable monomers [15] have been suggested. The comonomers widely used with 3-hydroxybutyrate in the study of PHA copolymers are 3-hydroxyvalerate to prepare poly(3-hydroxybutyrate-co-3-hydroxyvalerate) [16], 4-hydroxybutyrate to prepare poly(3-hydroxybutyrate-co-4-hydroxybutyrate) [17], and hydroxyhexanoate to prepare poly(3-hydroxybutyrate-co-hydroxyhexanoate) [18].

Due to the higher price of PHAs compared with commodity polymers, they have been considered for use in high priced medical materials, but the decrease in production costs through mass production is resulting in higher possibilities of extending its application to packaging material [19,20]. As a relatively smaller amount of PHA is needed to prepare foamed material with a porous structure, the development of packaging material from PHA using foaming agents is being carried out [21]. Polymer foams can be made by the addition of diverse chemical foaming agents [22,23], using environmentally friendly supercritical fluid in melt extrusion [24,25], and the introduction of supercritical fluid to beads in the solid state to prepare foam beads [26]. Obtained foam beads can be molded by chest injection molding [27]. There are two typical processes to produce bead foam, continuous process and batch process using foam extrusion and autoclave, respectively. In the autoclave bead, polymer beads are saturated with a physical blowing agent, and pressure in the autoclave is suddenly released to expand the beads. Bead foaming is an appropriate processing method for semi-crystalline polymers, such as polypropylene (PP) [28], polyurethane (TPU) [29], and PLA [30]. The use of carbon dioxide supercritical fluid to maintain the environmentally friendly nature of biodegradable polymers is reported mostly in PLA foams [31–35], and in the case of PHA, the melt extrusion foaming of PHBV with supercritical CO₂ is being carried out [36,37]. However, research on the foaming of P3HB has not been reported due to the lack of foamability. It is necessary to develop an eco-friendly supercritical CO₂ process using biodegradable P(3HB-co-4HB) with improved chain flexibility.

The effect of 4HB content in the bead foam process using supercritical CO₂ on the processing conditions and the resulting structure of the foams is studied. The effect of foaming temperature and pressure on the cell structure is studied in detail by evaluating the foam density, expansion ratio, etc. to explore the possibilities of application of these foams to packaging material. The effect of the addition of chain extending agents on the foam structure is also studied.

2. Experimental

The P(3HB-co-4HB) copolymer used in this study is a biodegradable polymer produced by CJ Cheiljedang, among which those with a 4HB content of 10–16% are confirmed to be crystalline and those with a 4HB content of 30 or 53.7% are confirmed to be non-crystalline. The chemical structure and 4HB content, along with molecular weights and heat of melting, are shown in Figure 1 and Table 1, respectively. A multifunctional styrene-acrylic oligomer (Joncryl, ADR 4370) purchased from BASF was used as a chain extender for the required control of the viscoelasticity of P(3HB-co-4HB) in the supercritical CO₂ foaming process.

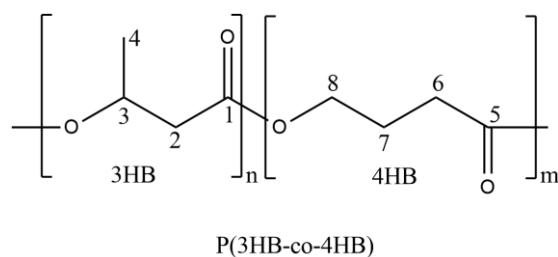


Figure 1. Chemical structure of P(3HB-co-4HB).

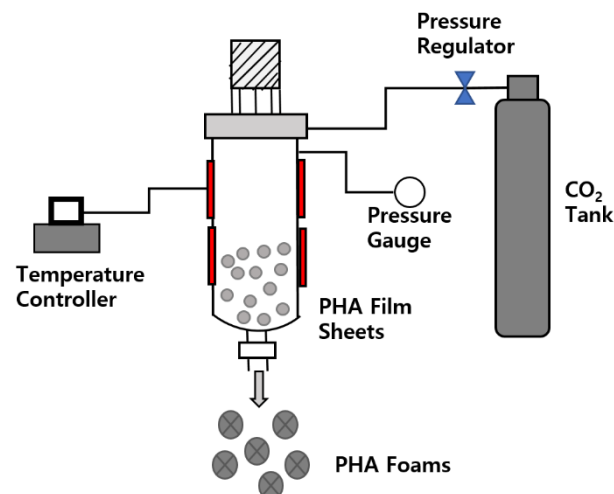
Table 1. Characteristics of P(3HB-co-4HB) used in this study.

| Sample Code [Polymer] | 4HB Content (%) | M _w (k) | ΔH _m (J/g) | T _{m1} (°C) | T _{m2} (°C) | T _c (°C) |
|---------------------------|-----------------|--------------------|-----------------------|----------------------|----------------------|---------------------|
| PHA10 [P(3HB-co-10% 4HB)] | 10 | 600 | 23.97 | 129.96 | 145.92 | 75.82 |
| PHA10 with ADR(5phr) | 10 | 600 | 9.65 | 113.59 | 141.96 | 72.53 |
| PHA10 [P(3HB-co-16% 4HB)] | 16 | 1000 | 3.99 | 115.82 | 155.59 | 59.67 |
| PHA10 with ADR(5phr) | 16 | 1000 | 2.54 | 113.55 | 154.96 | 56.84 |
| PHA10 [P(3HB-co-30% 4HB)] | 30 | 687 | - | - | - | - |
| PHA10 [P(3HB-co-50% 4HB)] | 53.7 | 901 | - | - | - | - |

P(3HB-co-4HB) of different 4HB contents were melt processed in an internal mixer (Haake, Rheomix600, Verden, Germany) at 20 rpm for 10 min at 140 °C, minimizing the thermal degradation to prepare samples of the same thermal history. When a 5 phr chain extender was added, the melt processing was carried out at 180 °C, which is the temperature at which the chain extender can react. The obtained P(3HB-co-4HB) samples were compression molded in a compression molding machine (QMESYS, QM900, Anyang, Korea) by heating at 140 °C for 2 min, raising the pressure to 8 MPa, and molded for 2 min, then quenched in water to obtain 1T thick 150 mm × 150 mm sheets. The sheets were cut into 5 mm × 5 mm pieces to use as beads for foaming.

The tan δ of P(3HB-co-4HB) was evaluated by measuring 1 mm × 2.5 mm sheets on a dynamic mechanical thermal analyzer (TA, DMA Q800/2980, New Castle, DE, USA) in the 30–140 °C range, at the oscillation frequency of 1 MHz.

The P(3HB-co-4HB) foam beads were prepared by adding 10 g of beads to a lab-made autoclave, as shown in Figure 2, diffusing supercritical CO₂ into P(3HB-co-4HB) for 60 min at the supercritical condition of CO₂ of 50–135 °C and 70–100 bar, then releasing the pressure abruptly to atmospheric pressure.

**Figure 2.** Schematic of supercritical CO₂ assisted foaming process.

The structure of the P(3HB-co-4HB) foams was evaluated with SEM pictures, taken on a scanning electron microscope (Hitachi, SEM S-5200, Hitachi, Tokyo, Japan) and by measuring the density before foaming (ρ_p) and the density after foaming (ρ_f) from which the expansion ratio (Φ) was calculated according to the following Equation (1).

$$\Phi = \frac{\rho_p}{\rho_f} \quad (1)$$

Cell density (N_f) refers to the number of cells (n) per cubic centimeter (A) in a foamed sample and can be defined by the following Equation (2).

$$N_f = \left(\frac{n}{A}\right)^{\frac{3}{2}} \times \Phi \quad (2)$$

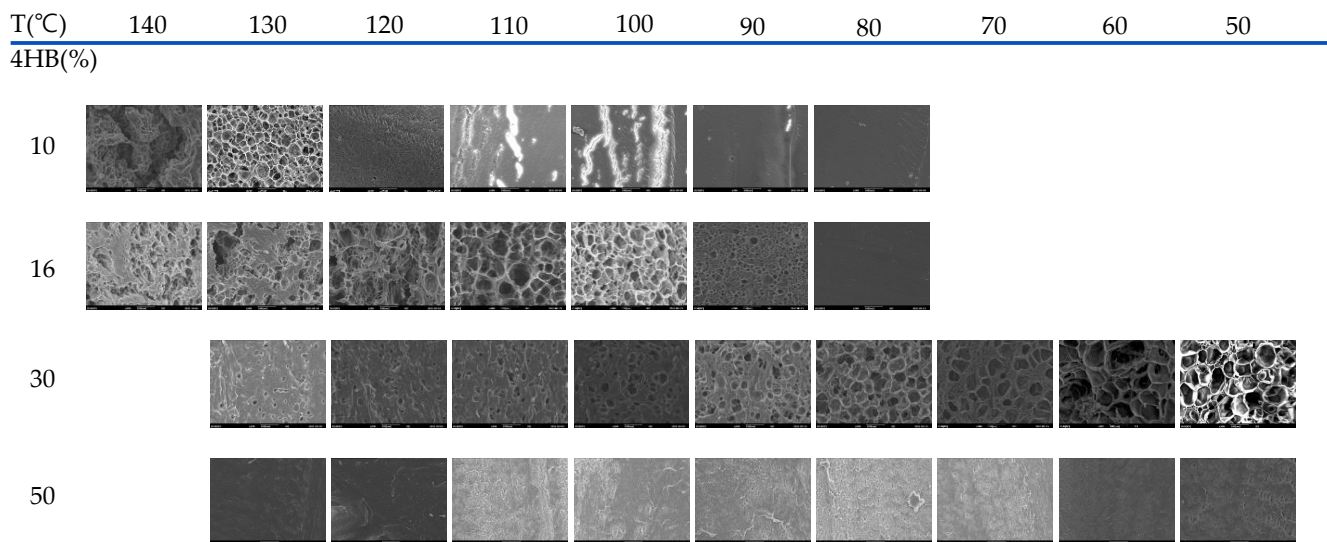
To measure the resilience rate of the crystalline P(3HB-co-10% 4HB) foam beads and noncrystalline P(3HB-co-30% 4HB) foam beads, the thickness of the foam beads was first determined as T_0 , then after compressing the foam beads to 50% its thickness and releasing the pressure after 30 min, the thickness was measured as T ; the resilience rate was calculated according to the following Equation (3).

$$R = \frac{T}{T_0} \times 100 (\%) \quad (3)$$

3. Results and Discussion

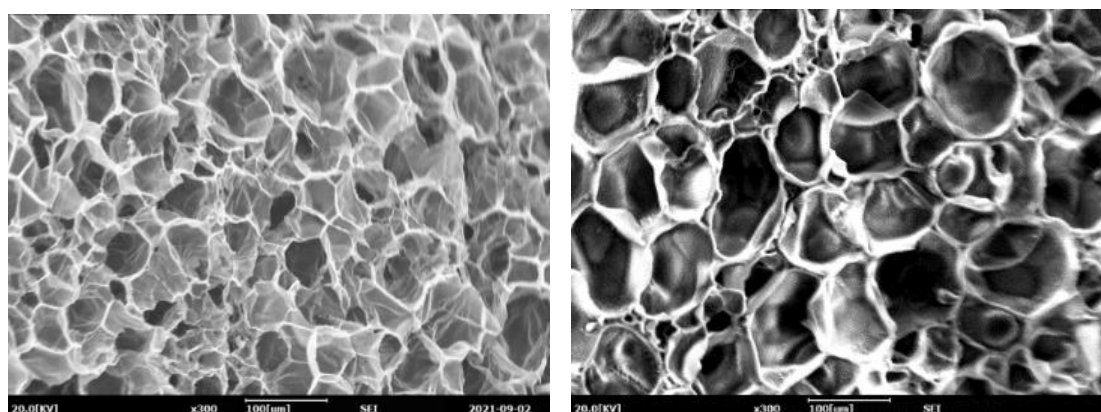
3.1. Foamability of P(3HB-co-4HB) Copolymer

The SEM micrographs that show the possibilities of cell formation in the foams prepared in the range 50–130 °C at 90 bar for different 4HB contents are shown in Figure 3. As can be observed, the temperature at which the cells develop depends on the 4HB content. In the case of P(3HB-co-10% 4HB), whose relative crystallinity is highest, (23.97 J/g) as shown in Table 1, cell structure develops when processed at 130 °C, while in the case of P(3HB-co-16% 4HB), whose relative crystallinity is lower (3.99 J/g), cell structure develops when processed at 100–110 °C. P(3HB-co-30% 4HB) is non-crystalline and the cell structure develops at a lower foaming temperature of 50–80 °C, but cell structure does not develop in the case of P(3HB-co-50% 4HB) in the range studied.



X300

Figure 3. Cont.



Open cell

Close cell

Figure 3. SEM micrographs of P(3HB-co-4HB) with different 4HB content foamed at 90 bar.

In supercritical foaming, the supercritical fluid diffuses into the polymer to create nuclei and they grow to form cells [38]. Nucleation and cell growth are affected by the crystalline/non-crystalline structure of the polymer and viscoelasticity, specifically, reasonable crystallinity and $\tan \delta$ value under the foaming conditions are required for nucleation and continuous growth of the cell. In crystalline P(3HB-co-4HB), poor solubility and diffusivity of CO_2 in crystallites caused the lowering of nucleation of the cell and prohibits cell growth, which resulted in less formability.

The change in $\tan \delta$ with temperature for the P(3HB-co-4HB) is shown in Figure 4. The $\tan \delta$ value and crystallinity are closely related to the chain mobility in the solid state. An increase in the $\tan \delta$ value is observed with an increase in temperature and 4HB content. The $\tan \delta$ is the ratio of loss modulus to storage modulus and shows a drastic change at various transition temperatures. The drastic change in the $\tan \delta$ with temperature can be observed as the temperature reaches the melting transition temperature of crystalline P(3HB-co-4HB) or the rubber transition temperature of non-crystalline P(3HB-co-4HB). The drastic change occurs at around 130 °C and 110 °C for crystalline P(3HB-co-10% 4HB) and P(3HB-co-16% 4HB), respectively, as their melting temperature depends on the 4HB content. On the other hand, the change can be observed above 50 °C and 30 °C for non-crystalline P(3HB-co-30% 4HB) and P(3HB-co-50% 4HB), respectively, where the mobility of the non-crystalline chains start to increase. The $\tan \delta$ value increases with 4HB content in P(3HB-co-4HB) and the change in the $\tan \delta$ value also increases at the respective transition temperatures. In the case of the P(3HB-co-4HB) copolymers, the chain mobility of 4HB is greater than that of 3HB, resulting in a higher $\tan \delta$ value and a more sensitive change with temperature. P(3HB-co-50% 4HB) exhibits a higher $\tan \delta$ value than other P(3HB-co-4HB) copolymers regardless of the temperature, due to the too much chain flexibility of the 4HB chain. The adequate $\tan \delta$ value required for cell growth in supercritical fluid foaming can be indirectly assessed by the $\tan \delta$ value reflecting the polymer's viscoelasticity. As observed in Figure 3, for copolymers with a 4HB content up to 30%, the $\tan \delta$ values below the transition temperature where the chains show a drastic change in their mobility are very similar, with the values being around 0.1. Therefore, foaming is expected to be possible below the transition where chain mobility is increased, which is 130 °C for P(3HB-co-10% 4HB), 110 °C for P(3HB-co-16% 4HB), and below 80 °C for P(3HB-co-30% 4HB). However, P(3HB-co-50% 4HB) exhibits a $\tan \delta$ value above 0.3, regardless of the temperature reflecting the extremely chain mobility; thus, cell growth in the foaming process is not possible. As observed in Figure 3, in the case of P(3HB-co-10% 4HB) of low 4HB content, the temperature range where foaming is possible is very narrow around 130 °C, as the stiffness of the chains is high, resulting in a drastic decrease in the mobility of chains. In the case of P(3HB-co-16% 4HB) where the flexibility of the chains is increased

with an increase in 4HB content, foaming is possible in a relatively broader temperature range of 100–110 °C, and P(3HB-co-30% 4HB), which has the highest chain mobility, has the widest window where foaming is possible of 50–90 °C. Therefore, it is evident that in non-crystalline P(3HB-co-4HB) an adequate $\tan \delta$ related to chain mobility above the glass transition temperature is an important factor in foaming.

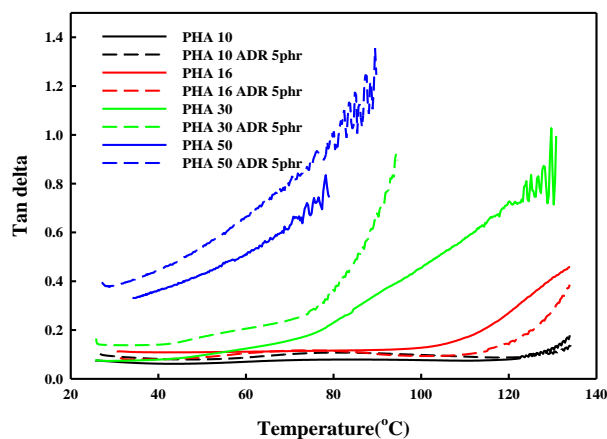


Figure 4. DMA thermograms of various P(3HB-co-4HB) with and without ADR.

3.2. Characteristics of P(3HB-co-4HB) Foams

The cell structure of P(3HB-co-4HB) foams shown in Figure 3 generally shows thinner cell walls, which hinder the formation of closed cells and result in an open cell structure compared with thermoplastic polyurethane (TPU) foam [39], which is highly elastic, and the cell size is also very irregular. However, the non-crystalline P(3HB-co-30% 4HB) foam exhibits thicker walls and more regular size in the closed cell, compared with crystalline P(3HB-co-4HB). This can be explained by the crystallinity and their morphology affecting the foaming temperature. In crystalline P(3HB-co-4HB), the chain flexibility to foam the cell can be obtained just under the melting temperature, and then the strength for cell nucleation and growth is rapidly lowered with a further increase in temperature, which resulted in uncontrolled cell growth and cell coalescence. However, cell growth and stabilization in non-crystalline P(3HB-co-4HB) are more stable because the forming could be archived in a broad range of temperatures with high elastic properties above the glass transition temperature. The cell structure is related to the resiliency against applied pressure. Figure 5 shows the resilience rate of the crystalline P(3HB-co-10% 4HB) foam and noncrystalline P(3HB-co-30% 4HB) foam. The resilience of P(3HB-co-30% 4HB), which is noncrystalline due to the high 4HB content, is greater than that of crystalline P(3HB-co-10% 4HB). This is due to the higher elasticity of P(3HB-co-30% 4HB) from its higher 4HB content and also due to the thicker cell walls and more regular cell structure. The resilience rate of P(3HB-co-30% 4HB) foamed at different temperatures, as shown in Figure 5b and showed much higher resilience for foams prepared at lower temperatures. This shows that the elastic properties of P(3HB-co-30% 4HB), along with open/close cell structure, the thickness of the cell walls, and cell size, which in turn depends on an expansion ratio, has a close relationship with resiliency. These results suggest that the possibility of using crystalline P(3HB-co-4HB) foams as an environmentally friendly packaging material is higher than that of using it for industrial structural material, which requires elasticity and resiliency to recover to its original form after compression, as it has an open cell structure compared with TPU foams. On the other hand, the non-crystalline P(3HB-co-30% 4HB) foams prepared at low temperatures with 100% resilience rates suggest the possibility of developing it as an industrial structural material.

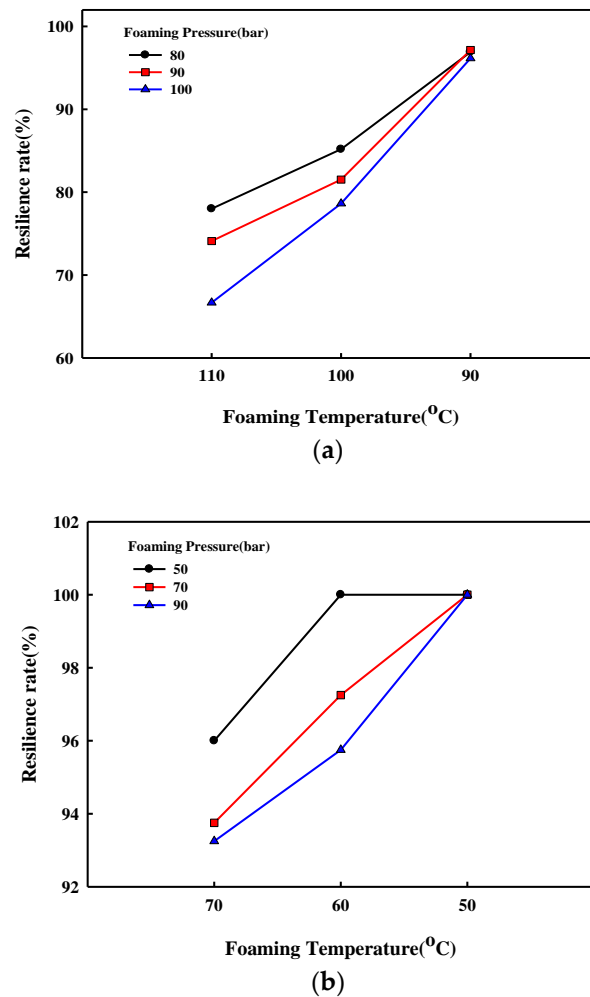


Figure 5. Resilience characteristics of P(3HB-co-4HB) foams; (a) crystalline P(3HB-co-16% 4HB); (b) non-crystalline P(3HB-co-30% 4HB).

Figure 6 shows the effect of foaming temperature on the density and the expansion rates calculated from density measurements before and after the expansion of P(3HB-co-4HB) beads of different 4HB content. The different foaming characteristic of P(3HB-co-30% 4HB) of different 4HB content was confirmed by the SEM micrographs in Figure 3. P(3HB-co-50% 4HB) with the highest 4HB content does not show a significant change in density over the range studied, suggesting that cell growth from the diffused supercritical CO₂ is not possible, due to its high $\tan \delta$ value. The growth of cells in P(3HB-co-30% 4HB) at the foaming temperatures of 50–80 °C due to adequate $\tan \delta$ and chain mobility can be confirmed. The cell growth of crystalline P(3HB-co-10% 4HB) and P(3HB-co-16% 4HB) at low temperatures is difficult due to the crystalline structure and lack of chain mobility, but near the melting temperature, chain mobility occurs and the $\tan \delta$ becomes adequate for foaming to result in cell growth. The highest expansion ratios are obtained at 130 °C and 110 °C for P(3HB-co-10% 4HB) and P(3HB-co-16% 4HB), respectively. However, the uniformity of cells is very poor, due to the rapid decrease in strength to maintain cells during the stabilization step. The expansion ratio of non-crystalline P(3HB-co-30% 4HB) is below 6, while that of crystalline P(3HB-co-10% 4HB) and P(3HB-co-16% 4HB) is over 20. These P(3HB-co-4HB) foams have different expansion ratios, suggesting that they can be used to prepare foams for different applications.

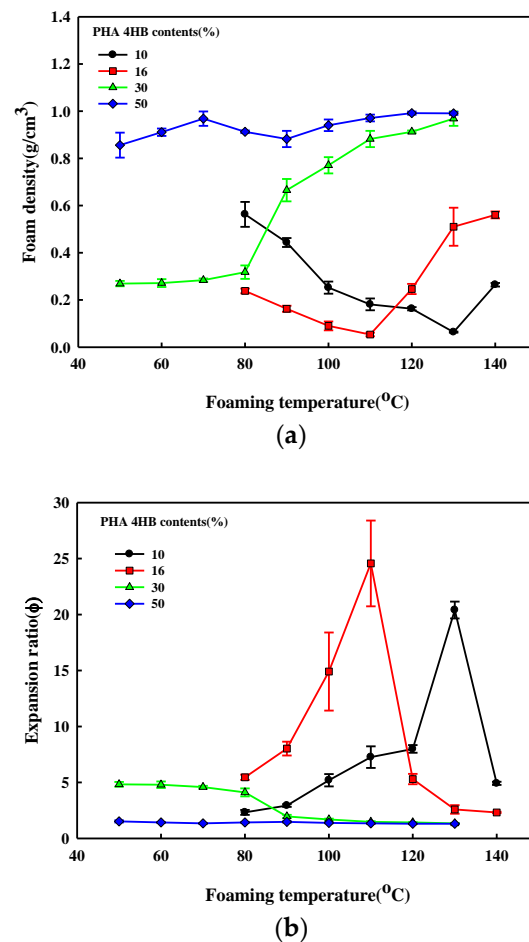


Figure 6. Effect of foaming temperature on the structure of the P(3HB-co-4HB) bead foamed at 90 bar; (a) foam density; (b) expansion ratio.

The effect of foaming pressure on foam formation of P(3HB-co-4HB) is shown in Figure 7. The foaming temperature was set at the temperature at which the maximum expansion ratio could be obtained from the respective P(3HB-co-4HB) at 90 bar. The cell size increases with the increase in pressure. The foam density and expansion ratio of the P(3HB-co-4HB) copolymers shown in Figure 8 show a decrease in the foam density and an increase in the expansion ratio with an increase in pressure. An increase in the foaming pressure allows more diffusion of supercritical CO₂ into P(3HB-co-4HB) to form a greater number of nuclei in P(3HB-co-4HB) beads, which results in a decrease in the foam density and an increase in the expansion ratio on cell growth when the pressure is relieved. This effect of pressure is more evident in the higher 4HB content P(3HB-co-4HB), showing that diffusion of the supercritical CO₂ is easier in the non-crystalline P(3HB-co-4HB) than the crystalline P(3HB-co-4HB).

3.3. Effect of Chain Extender on Foam Structures

SEM micrographs that show the effect of the addition of a chain extender on the supercritical CO₂ foaming are shown in Figure 9. Although the addition of a chain extender to crystalline P(3HB-co-10% 4HB) increases cell size when foamed at 130 °C, it does not affect the temperature window where foaming is possible, while in the case of P(3HB-co-16% 4HB), the temperature window appears at a higher temperature and is broadened from 110–100 °C to 120–130 °C. Figure 8b shows that although foaming of non-crystalline P(3HB-co-30% 4HB) is possible in the temperature range 50–90 °C in the absence of a chain extender, it is not when a chain extender is added. It was found that the degree of crystallinity of P(3HB-co-4HB) modified by a chain extender decreased dramatically,

as shown in Table 1. This indicated that the crystalline structural change and the chain flexibility took place by chemical modification. As a result, the $\tan \delta$ decreases observed in Figure 4 are caused by a structural change in the formation of chain branching or crosslinking from the reaction of epoxy groups of the chain extender Joncryl ADR 4370, containing epoxy groups, and the 3HB hydroxy groups in the crystalline P(3HB-co-4HB) of low 4HB content, resulting in a decrease in $\tan \delta$. However, in the case of P(3HB-co-4HB) of high 4HB content, viscosity decrease occurs instead of the aforementioned increase and decreases $\tan \delta$ to decrease the foamability. Figure 10 shows the effect of a chain extender on the foam density and expansion ratio of the foam. The addition of the chain extender does not affect the foaming conditions in the case of P(3HB-co-10% 4HB) due to relatively high crystallinity, but a general increase in the expansion ratio with a decrease in foam density occurs. However, in the case of P(3HB-co-16% 4HB), the change in $\tan \delta$ with the change in the chain structure allows foaming at temperatures above 110 °C and the foam density remains low above 110 °C to allow foaming at 120–130 °C, where foaming was not possible in the absence of a chain extender and an expansion ratio of around 20 can be obtained. Therefore, the control of the foaming properties with a chain extender is only possible in crystalline P(3HB-co-16% 4HB) with reasonably low crystallinity and $\tan \delta$ value.

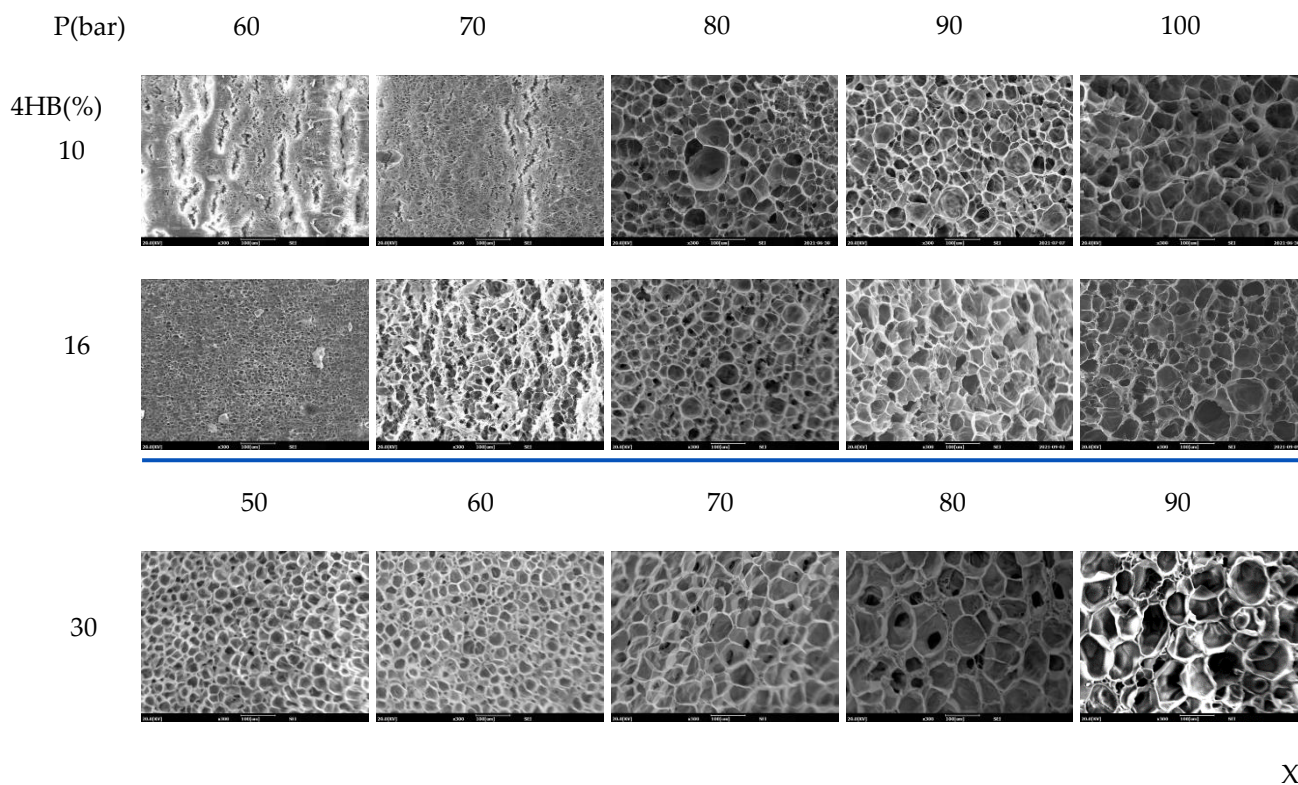


Figure 7. SEM micrographs of P(3HB-co-4HB) foamed at various foaming pressure. Foaming temperatures of P(3HB-co-10% 4HB), P(3HB-co-16% 4HB), and P(3HB-co-30% 4HB) are 130 °C, 100 °C, 50 °C, respectively.

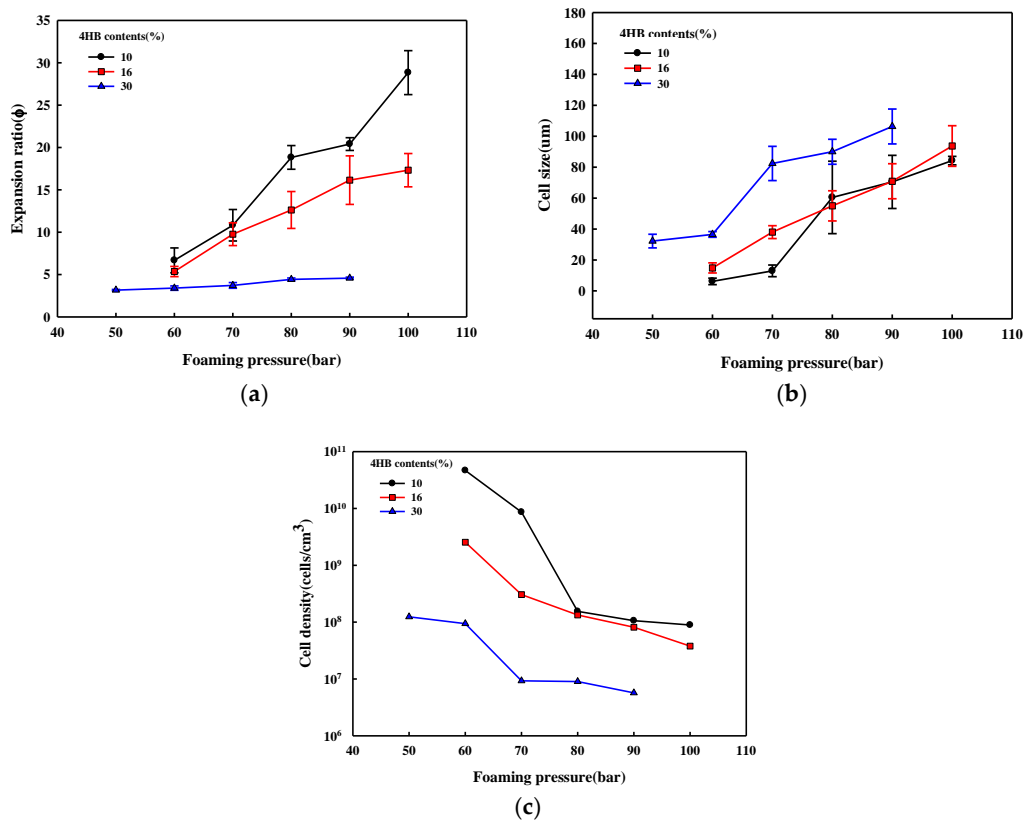
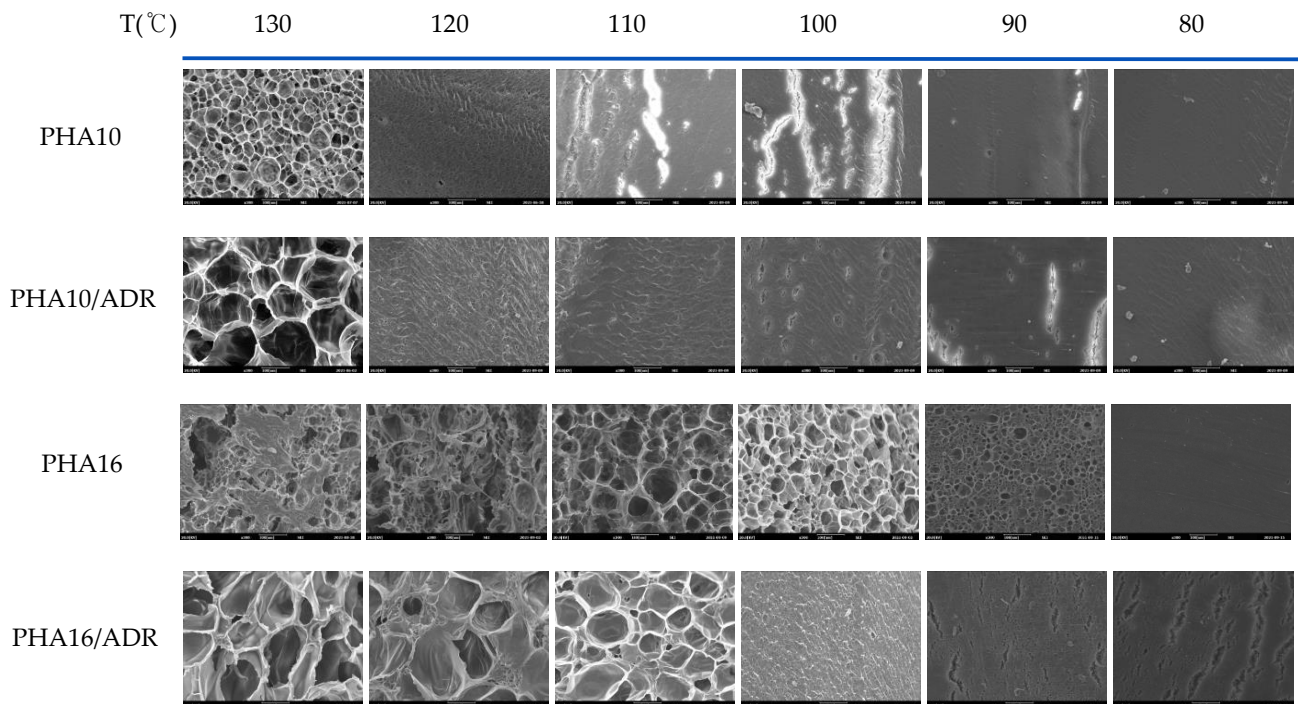


Figure 8. Effect of forming pressure on the structure of the P(3HB-co-4HB) foams. Foaming temperatures of P(3HB-co-10% 4HB), P(3HB-co-16% 4HB), and P(3HB-co-30% 4HB) are 130 °C, 100 °C, 50 °C, respectively; (a) expansion ratio; (b) cell size; (c) cell density.



X300

Figure 9. SEM micrographs of foamed crystalline P(3HB-co-4HB) with and without chain extender.

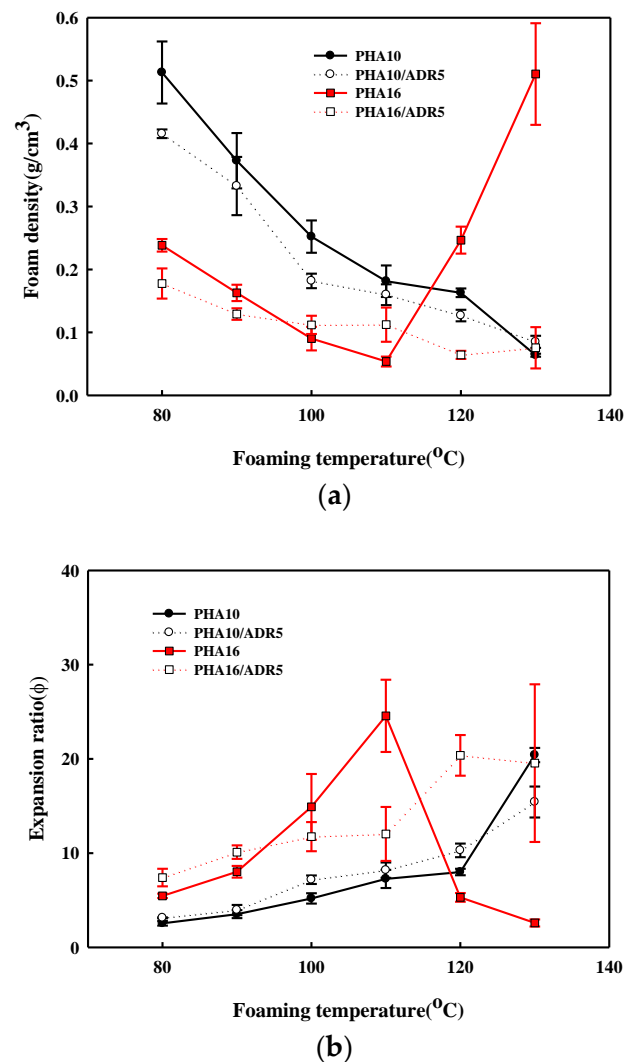


Figure 10. Effect of chain extender on the structure of the P(3HB-co-4HB) foams; (a) foam density; (b) expansion ratio.

4. Conclusions

Biodegradable P(3HB-co-4HB) of different 4HB contents and foam beads processed with supercritical carbon dioxide was used to study the effects of 4HB content on the foaming conditions and foam properties. It was found that various foam structures for packaging and industrial materials were obtained by controlling the 4HB content in P(3HB-co-4HB), which resulted in changes in the crystallinity and viscoelastic properties of P(3HB-co-4HB). The low 4HB content P(3HB-co-4HB) that maintained a crystalline structure can be foamed just under the melting temperature, but the range of the foaming temperature becomes broader with an increase in the 4HB content. The expansion ratio is around 20 and an open cell structure is formed. The non-crystalline P(3HB-co-4HB) of high 4HB content has a relatively wide window of foaming around the temperature at which chain mobility occurs. The formed foam has thicker cell walls, expansion ratios of about 6, and the cell size is regular, resulting in enhanced resiliency against compression, compared with crystalline P(3HB-co-4HB). The chain extender changes the chain structure of crystalline P(3HB-co-16% 4HB), which changes the crystallinity and chain mobility and, thus, changes the temperature at which foaming is possible and the cell structure. To enhance the physical properties of P(3HB-co-4HB) foams, future studies for the blends and composites using P(3HB-co-4HB) may be considered.

Author Contributions: Conceptualization, H.-J.K.; investigation, T.Z., E.L. and Y.J.; writing—original draft, T.Z. and H.-J.K.; funding acquisition, E.L. and S.S. All authors have read and agreed to the published version of the manuscript.

Funding: CJ Cheiljedang.

Institutional Review Board Statement: Not applicable.

Informed Consent Statement: Informed consent was obtained from all the subjects involved in the study.

Data Availability Statement: Data are in the authors' possession.

Conflicts of Interest: The authors declare no conflict of interest.

References

1. Chen, G.Q. A microbial polyhydroxyalkanoates (PHA) based bio- and materials industry. *Chem. Soc. Rev.* **2009**, *38*, 2434–2446. [[CrossRef](#)] [[PubMed](#)]
2. Ong, S.Y.; Chee, J.Y.; Sudesh, K. Degradation of Polyhydroxyalkanoate (PHA): A Review. *J. Sib. Fed. Univ. Biol.* **2017**, *10*, 211–225. [[CrossRef](#)]
3. Puppi, D.; Pecorini, G.; Chiellini, F. Biomedical Processing of Polyhydroxyalkanoates. *Bioengineering* **2019**, *6*, 0108. [[CrossRef](#)] [[PubMed](#)]
4. Thellen, C.; Coyne, M.; Froio, D.; Auerbach, M.; Wirsén, C.; Ratto, J.A. A Processing. Characterization and Marine Biodegradation Study of Melt-Extruded Polyhydroxyalkanoate (PHA) Films. *J. Polym. Environ.* **2008**, *16*, 1–11. [[CrossRef](#)]
5. Vostrejs, P.; Adamcova, D.; Vavrkova, M.D.; Enev, V.; Kalina, M.; Machovsky, M.; Sourkov, M.; Marovaa, I.; Kovalcik, A. Active biodegradable packaging films modified with grape seeds lignin. *RSC Adv.* **2020**, *10*, 29202–29213. [[CrossRef](#)]
6. Cravo, C.; Duarte, A.R.C.; Duarte, C.M.M. Solubility of carbon dioxide in a natural biodegradable polymer: Determination of diffusion coefficients. *J. Supercrit. Fluids* **2007**, *740*, 194–199. [[CrossRef](#)]
7. Volova, T.; Goncharov, D.; Sukovatyi, A.; Shabanov, A.; Nikolaeva, E.; Shishatskaya, E. Electrospinning of polyhydroxyalkanoate fibrous scaffolds: Effects on electrospinning parameters on structure and properties. *J. Biomater. Sci. Polym. Ed.* **2013**, *25*, 370–393. [[CrossRef](#)]
8. Grande, D.; Ramier, J.; Versace, D.L.; Renard, E.; Langlois, V. Design of functionalized biodegradable PHA-based electrospun scaffolds meant for tissue engineering applications. *New Biotechnol.* **2017**, *37*, 129–137. [[CrossRef](#)]
9. Thomas, S.; Shumilova, A.A.; Kiselev, E.G.; Baranovsky, S.V.; Vasiliev, A.D.; Nemtsev, I.V.; Kuzmin, A.P.; Sukovatyi, A.G.; Avinash, R.P.; Volova, T.G. Thermal, mechanical and biodegradation studies of biofiller based poly-3-hydroxybutyrate biocomposites. *Int. J. Biol. Macromol.* **2020**, *155*, 1373–1384. [[CrossRef](#)]
10. Che, X.M.; Ye, H.M.; Chen, G.Q. Effects of uracil on crystallization and rheological property of poly(R-3-hydroxybutyrate-co-4-hydroxybutyrate). *Compos. A Appl. Sci. Manuf.* **2018**, *109*, 141–150. [[CrossRef](#)]
11. Sun, J.Y.; Shen, J.J.; Chen, S.K.; Cooper, M.A.; Fu, H.B.; Wu, D.M.; Yang, Z.G. Nanofiller Reinforced Biodegradable PLA/PHA Composites: Current Status and Future Trends. *Polymers* **2018**, *10*, 0505. [[CrossRef](#)] [[PubMed](#)]
12. Parulekar, Y.; Mohanty, A.K. Extruded Biodegradable Cast Films from Polyhydroxyalkanoate and Thermoplastic Starch Blends: Fabrication and Characterization. *Macromol. Mater. Eng.* **2007**, *292*, 1218–1228. [[CrossRef](#)]
13. Musiol, M.; Jurczyk, S.; Sobota, M.; Klim, M.; Sikorska, W.; Zieba, M.; Janeczek, H.; Rydz, J.; Kurcok, P.; Johnston, B.; et al. (Bio)Degradable Polymeric Materials for Sustainable Future—Part 3: Degradation Studies of the PHA/Wood Flour-Based Composites and Preliminary Tests of Antimicrobial Activity. *Materials* **2020**, *13*, 2200. [[CrossRef](#)] [[PubMed](#)]
14. Ventura, H.; Laguna-Gutierrez, E.; Rodriguez-Perez, M.A.; Ardanuy, M. Effect of chain extender and water-quenching on the properties of poly(3-hydroxybutyrate-co-4-hydroxybutyrate) foams for its production by extrusion foaming. *Eur. Polym. J.* **2016**, *85*, 14–25. [[CrossRef](#)]
15. Li, S.Y.; Dong, C.L.; Wang, S.Y.; Ye, H.M.; Chen, G.Q. Microbial production of polyhydroxyalkanoate block copolymer by recombinant *Pseudomonas putida*. *Appl. Microbiol. Biotechnol.* **2010**, *90*, 659–669. [[CrossRef](#)]
16. Ahankari, S.S.; Mohanty, A.K.; Misra, M. Mechanical behaviour of agro-residue reinforced poly(3-hydroxybutyrate-co-3-hydroxyvalerate), (PHBV) green composites: A comparison with traditional polypropylene composites. *Compos. Sci. Technol.* **2011**, *71*, 653–657. [[CrossRef](#)]
17. Al-Kaddo, K.B.; Mohamad, F.; Murugan, P.; Tan, J.S.; Sudesh, K.; Samian, M.R. Production of P(3HB-co-4HB) copolymer with high 4HB molar fraction by *Burkholderia contaminans* Kad1 PHA synthase. *Biochem. Eng. J.* **2020**, *153*, 107394–107400. [[CrossRef](#)]
18. Tripathi, L.; Wu, L.P.; Chen, J.C.; Chen, G.Q. Synthesis of Diblock copolymer poly-3-hydroxybutyrate -block-poly-3-hydroxyhexanoate [PHB-b-PHHx] by a β -oxidation weakened *Pseudomonas putida* KT2442. *Microb. Cell. Factories* **2012**, *11*, 44–54. [[CrossRef](#)]
19. Vijayendra, S.V.N.; Shamala, T.R. Film forming microbial biopolymers for commercial applications—A review. *Crit. Rev. Biotechnol.* **2014**, *34*, 338–357. [[CrossRef](#)]

20. Zhang, J.Q.; Kasuya, K.; Hikima, T.; Takata, M.; Takemura, A.; Lwata, T. Mechanical properties, structure analysis and enzymatic degradation of uniaxially cold-drawn films of poly[(R)-3-hydroxybutyrate-co-4-hydroxybutyrate]. *Polym. Degrad. Stab.* **2011**, *96*, 2130–2138. [[CrossRef](#)]
21. Plackett, D.; Siro, I. Polyhydroxyalkanoates (PHAs) for food packaging. *Multifunct. Nanoreinforced Polym. Food Packag.* **2011**, *4*, 498–526.
22. Liao, Q.; Tsui, A.; Billington, S.; Frank, C.W. Extruded Foams from Microbial Poly(3-hydroxybutyrate-co-3-hydroxyvalerate) and Its Blends with Cellulose Acetate Butyrate. *Polym. Eng. Sci.* **2012**, *52*, 1495–1508. [[CrossRef](#)]
23. Wright, Z.C.; Frank, C.W. Increasing Cell Homogeneity of Semicrystalline, Biodegradable Polymer Foams with a Narrow Processing Window via Rapid Quenching. *Polym. Eng. Sci.* **2014**, *54*, 2877–2886. [[CrossRef](#)]
24. Moigne, N.L.; Sauceau, M.; Benyakhlef, M.; Jemai, R.; Benezet, J.C.; Rodier, E.; Lopez-Cuesta, J.M.; Fages, J. Foaming of poly(3-hydroxybutyrate-co-3-hydroxyvalerate)/organo-clays nano-biocomposites by a continuous supercritical CO₂ assisted extrusion process. *Eur. Polym. J.* **2014**, *61*, 157–171. [[CrossRef](#)]
25. Takahashi, S.; Hassler, J.C.; Kiran, E. Melting behavior of biodegradable polyesters in carbon dioxide at high pressures. *J. Supercrit. Fluids* **2012**, *72*, 278–287. [[CrossRef](#)]
26. Ke, J.; Zhang, L.; Li, D.L.; Bao, J.B.; Wang, Z.B. Foaming of Poly(3-hydroxybutyrate-co-3-hydroxyvalerate) with Supercritical Carbon Dioxide: Foaming Performance and Crystallization Behavior. *ACS Omega* **2020**, *5*, 9839–9845.
27. Ge, C.B.; Ren, Q.; Wang, S.P.; Zheng, W.G.; Zhai, W.T.; Park, C.B. Steam-chest molding of expanded thermoplastic polyurethane bead foams and their mechanical properties. *Chem. Eng. Sci.* **2017**, *17*, 337–346. [[CrossRef](#)]
28. Hossieny, N.; Ameli, A.; Park, C.B. Characterization of Expanded Polypropylene Bead Foams with Modified Steam-Chest Molding. *Ind. Eng. Chem. Res.* **2013**, *52*, 8236–8247. [[CrossRef](#)]
29. Jiang, J.J.; Liu, F.; Yang, X.; Xiong, Z.J.; Liu, H.W.; Xu, D.H.; Zhai, W.T. Evolution of ordered structure of TPU in high-elastic state and their influences on the autoclave foaming of TPU and inter-bead bonding of expanded TPU beads. *Polymer* **2021**, *228*, 123872–123884. [[CrossRef](#)]
30. Tang, L.Q.; Zhai, W.T.; Zheng, W.G. Autoclave preparation of expanded polypropylene/poly(lactic acid) blend bead foams with a batch foaming process. *J. Cell. Plast.* **2011**, *47*, 429–446. [[CrossRef](#)]
31. Gong, P.J.; Zhai, S.; Lee, R.; Zhao, C.X.; Buahom, P.; Li, G.X.; Park, C.B. Environmentally Friendly Polylactic Acid-Based Thermal Insulation Foams Blown with Supercritical CO₂. *Ind. Eng. Chem. Res.* **2015**, *57*, 5464–5471. [[CrossRef](#)]
32. Yang, Y.C.; Li, X.Y.; Zhang, Q.Q.; Xia, C.H.; Chen, C.; Chen, X.H.; Yu, P. Foaming of poly(lactic acid) with supercritical CO₂: The combined effect of crystallinity and crystalline morphology on cellular structure. *J. Supercrit. Fluids* **2019**, 145122–145132. [[CrossRef](#)]
33. Nofar, M.; Park, C.B. Poly(lactic acid)foaming. *Prog. Polym. Sci.* **2014**, *39*, 1721–1741. [[CrossRef](#)]
34. Standau, T.; Zhao, C.J.; Castellon, S.M.; Bonten, C.; Altstadt, V. Chemical Modification and Foam Processing of Polylactide (PLA). *Polymers* **2019**, *11*, 0306. [[CrossRef](#)]
35. Szegda, D.; Duangphet, S.; Song, J.; Tarverdi, K. Extrusion foaming of PHBV. *J. Cell. Plast.* **2014**, *50*, 145–162. [[CrossRef](#)]
36. Javadi, A.; Srithep, Y.; Clemons, C.C.; Turng, L.S.; Gong, S.Q. Processing of poly(hydroxybutyrate-co-hydroxyvalerate)-based bionanocomposite foams using supercritical fluids. *J. Mater. Res.* **2012**, *27*, 1506–1517. [[CrossRef](#)]
37. Frerich, S.C. Biopolymer foaming with supercritical CO₂—Thermodynamics, foaming behaviour and mechanical characteristics. *J. Supercrit. Fluids* **2015**, *96*, 349–358. [[CrossRef](#)]
38. Banerjee, R.; Ray, S.S. Foamability and Special Applications of Microcellular Thermoplastic Polymers: A Review on Recent Advances and Future Direction. *Macromol. Mater. Eng.* **2020**, *305*, 2000366–2000414. [[CrossRef](#)]
39. Zhang, T.; Lee, S.J.; Yoo, Y.H.; Park, K.H.; Kang, H.J. Compression Molding of Thermoplastic Polyurethane Foam Sheets with Beads Expanded by Supercritical CO₂ Foaming. *Polymers* **2021**, *13*, 0656. [[CrossRef](#)]